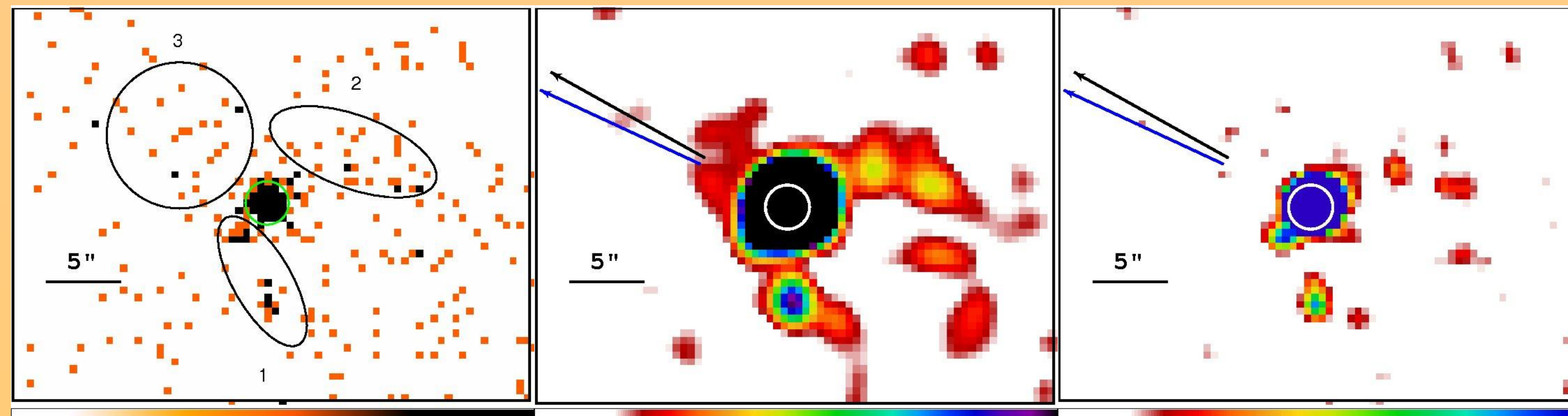


Pulsar B1929+10 and its environment

Zdenka Misanovic, George Pavlov, & Gordon Garmire (Penn State)

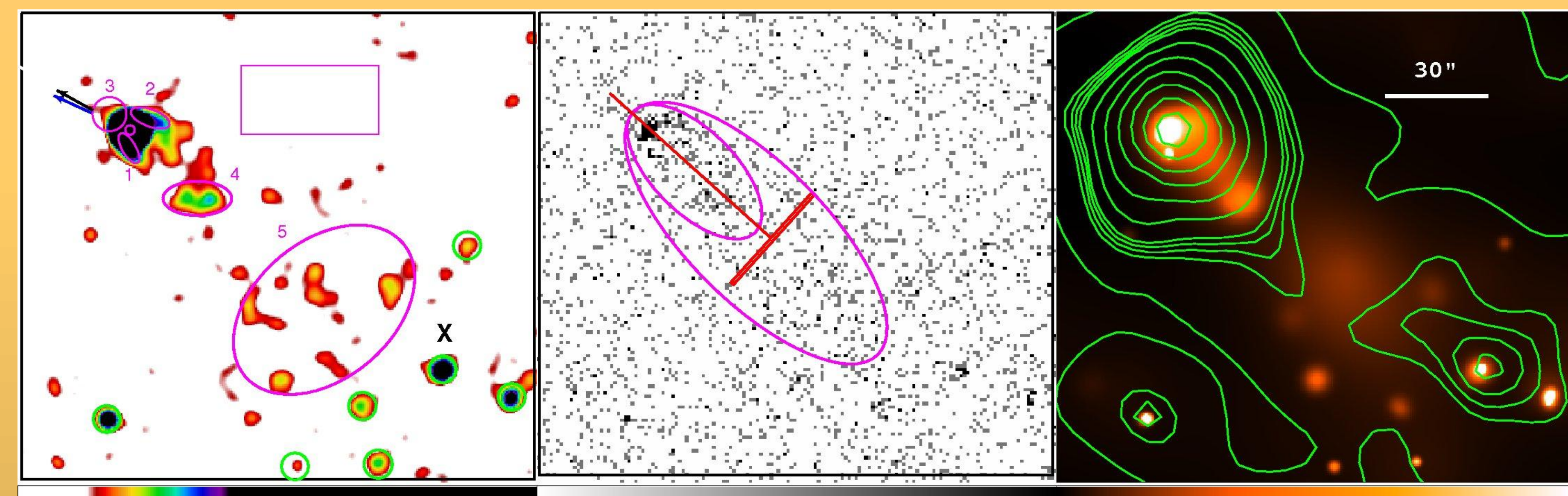
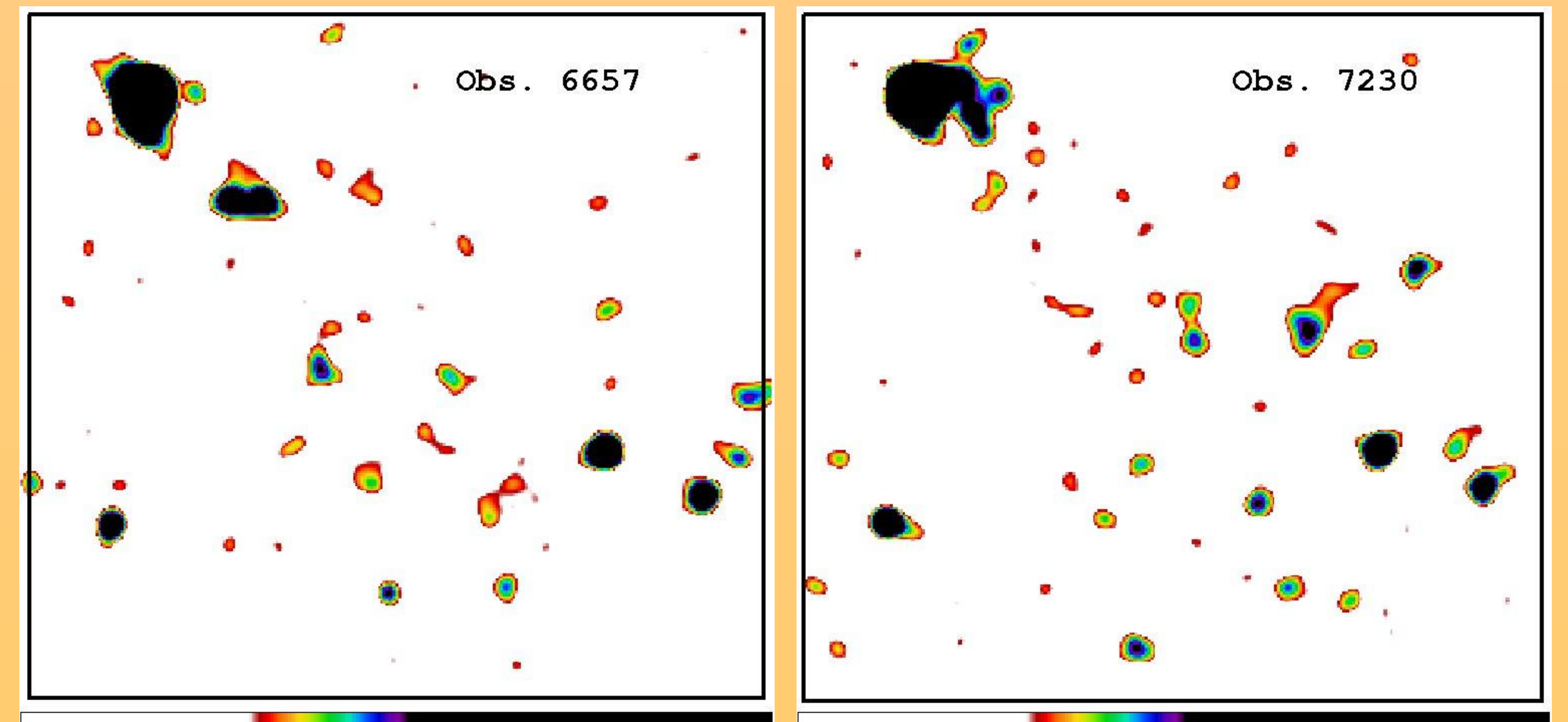
We report on two Chandra observations of B1929+10, which reveal a PWN with a torus bent in the direction opposite to the pulsar's proper motion and possibly a small jet in the immediate vicinity of this 3-Myr-old pulsar. There is also a long tail behind the pulsar, extending up to 2' in Chandra images and ~15' in the XMM-Newton data, with a luminosity of ~10e30 ergs/s in the 0.3-8 keV band. However, the PWN morphology does not seem to be entirely consistent with the existing MHD simulations for bow-shock PWNe, suggesting that the intrinsic anisotropy of the pulsar wind must be taken into account when modeling such objects. Contrary to previous results, our spectral analysis suggests that, in addition to the magnetospheric emission, there is a strong thermal component (~40-50% of the total emission in the 0.3-10 keV band) in the pulsar's spectrum. The combined Chandra and XMM-Newton data suggest that the thermal emission emerges from a polar cap region with an apparent radius of ~30-40 m and a temperature of about 0.3 keV.



Images of the field around B1929 in the 0.3--8 keV band, combining two ACIS-S3 observations (6657 and 7230). Left: unsmoothed image (pixel size is 0.492''). The circular and elliptical regions mark the smallest structures detected around the pulsar at approximately 3 σ levels in at least one of the observations. Middle: The same image smoothed using a Gaussian of FWHM 1''. The blue arrow shows the direction of the measured pulsar's proper motion, while the black arrow indicates the proper motion corrected for the Galactic rotation and solar peculiar velocity. Right: In this image the pulsar contribution is subtracted and smoothing with a Gaussian of FWHM 0.5'' is applied. The brightness scales in the middle and right panels are selected to emphasize different components of the extended emission in the vicinity of B1929. The position of the pulsar is indicated by a 1.5'' circle in all the panels.

POSSIBLE VARIABILITY:

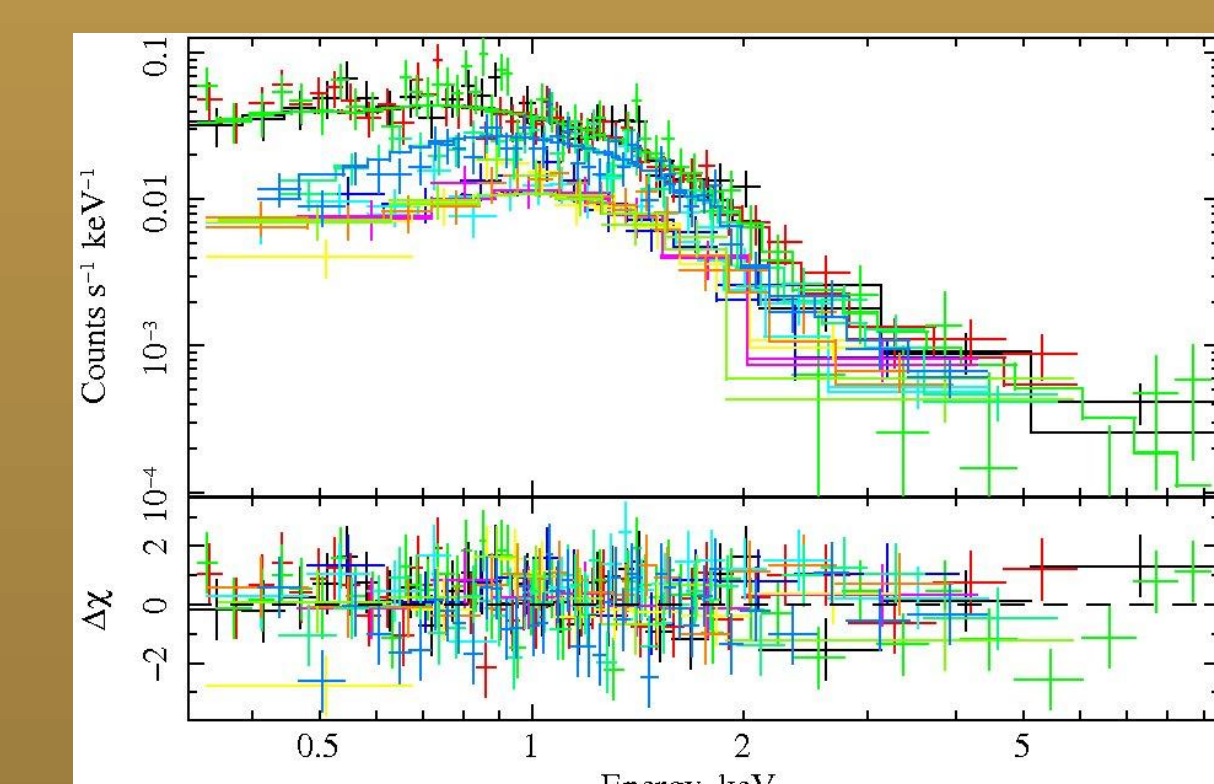
Top: 0.3-8 keV images of the first (left) and second (right) ACIS-S3 observations, smoothed using a Gaussian of FWHM 2''. Bottom: The same images adaptively smoothed to show the structures with the signal-to-noise ratio in the range 2.2 to 4.



Left: ACIS-S3 image of B1929+10 and its environment produced by combining observations 6657 and 7230, in the 0.3--8 keV band. The unbinned image is smoothed using a Gaussian of FWHM 2''. The elliptical regions mark the smallest structures detected around B1929+10. The pulsar's position is marked by a 1.5'' circle, while the 40'' x 20'' box shows the region used for the background evaluation. The unbinned image is smoothed using a Gaussian of FWHM 2''. The arrows indicate the direction of the pulsar's proper motion (measured and corrected). The green circles enclose possible faint point sources in the field of view (X marks the source found with CELLDetect). Middle: unsmoothed 0.3-8 keV combined image showing the same region. The image is binned by a factor of two. The two ellipses show the largest regions of enhanced emission, in which the diffuse emission is detected at a $\approx 10\sigma$ level. Right: The same unbinned image smoothed using an adaptive Gaussian kernel with the size self-adjusting to show the structures with the signal-to-noise ratio in the range 2.2 to 4. The overlaid contours correspond to the combined XMM-Newton observations.

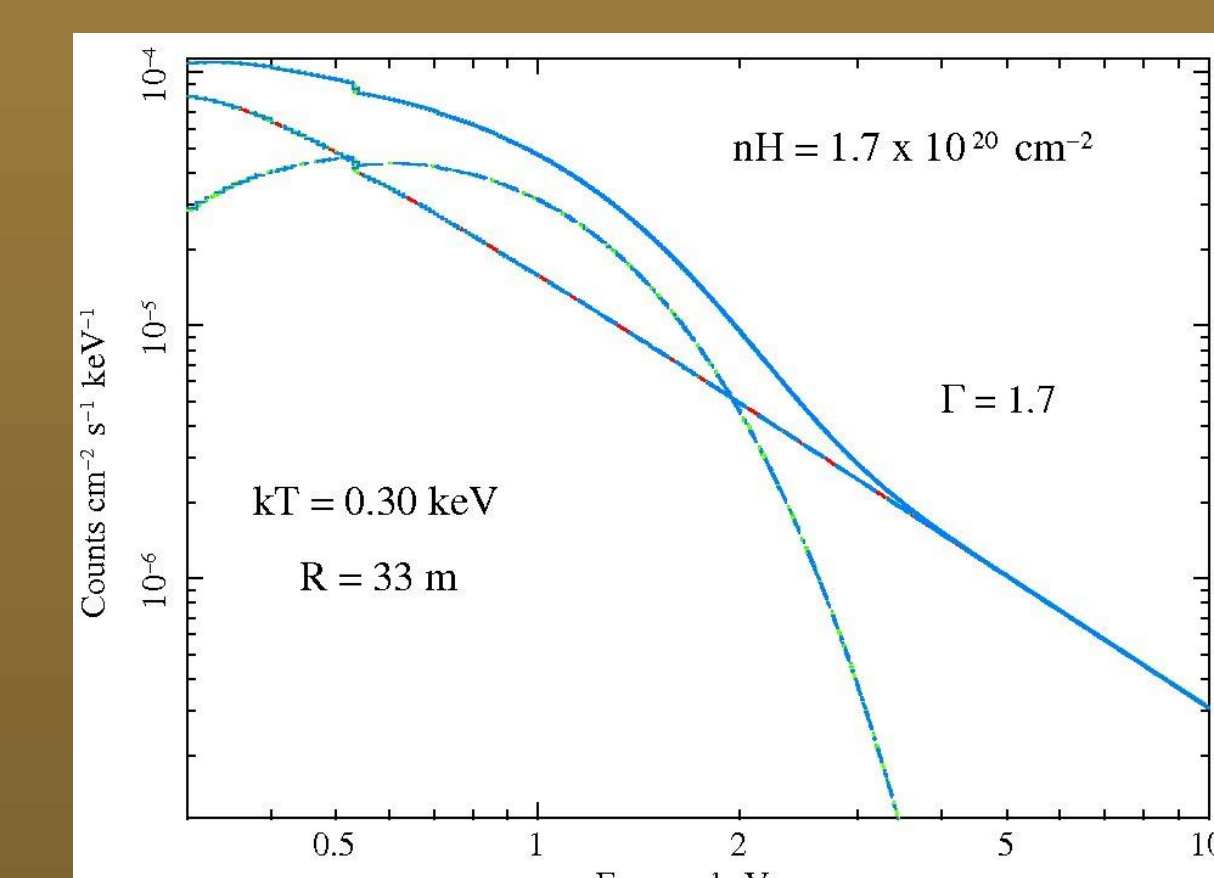


To interpret the B1929+10 PWN in the framework of the current MDH models, we attempted to match the observed morphological structures with those predicted by the simulations. However, the comparison leads to some discrepancies. For example, the predicted length of the pulsar tail would be ~150 pc, which is two orders of magnitude larger than observed by XMM-Newton and ROSAT. The main reason is the assumption of the model that the flow speed remains very high along the entire tail. Bucciantini et al. (2005) suggest that the flow can be slowed down by the interaction with the ISM. We estimated that the flow velocity of ~0.09c would be required to match the observed tail length of ~1.5 pc. This velocity is still much larger than the velocity of the pulsar.



THE X-RAY SPECTRUM OF B1929+10

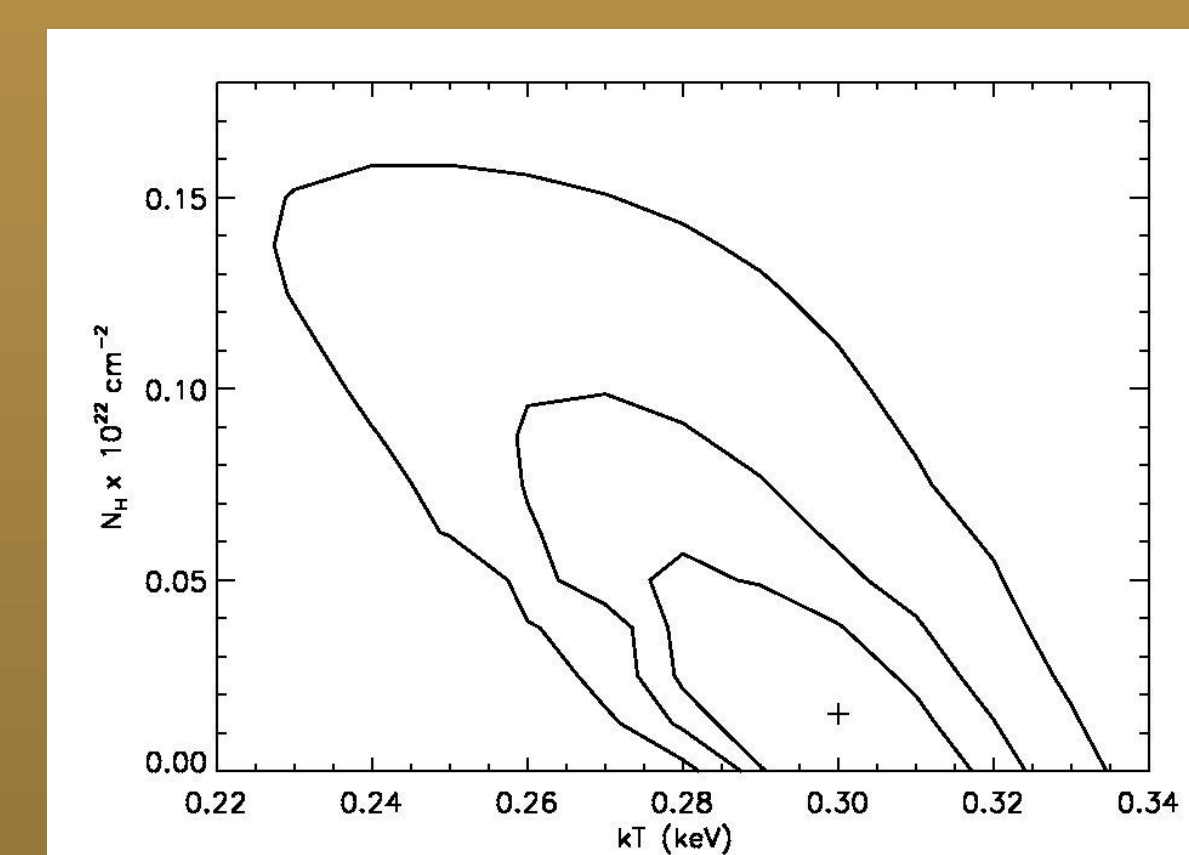
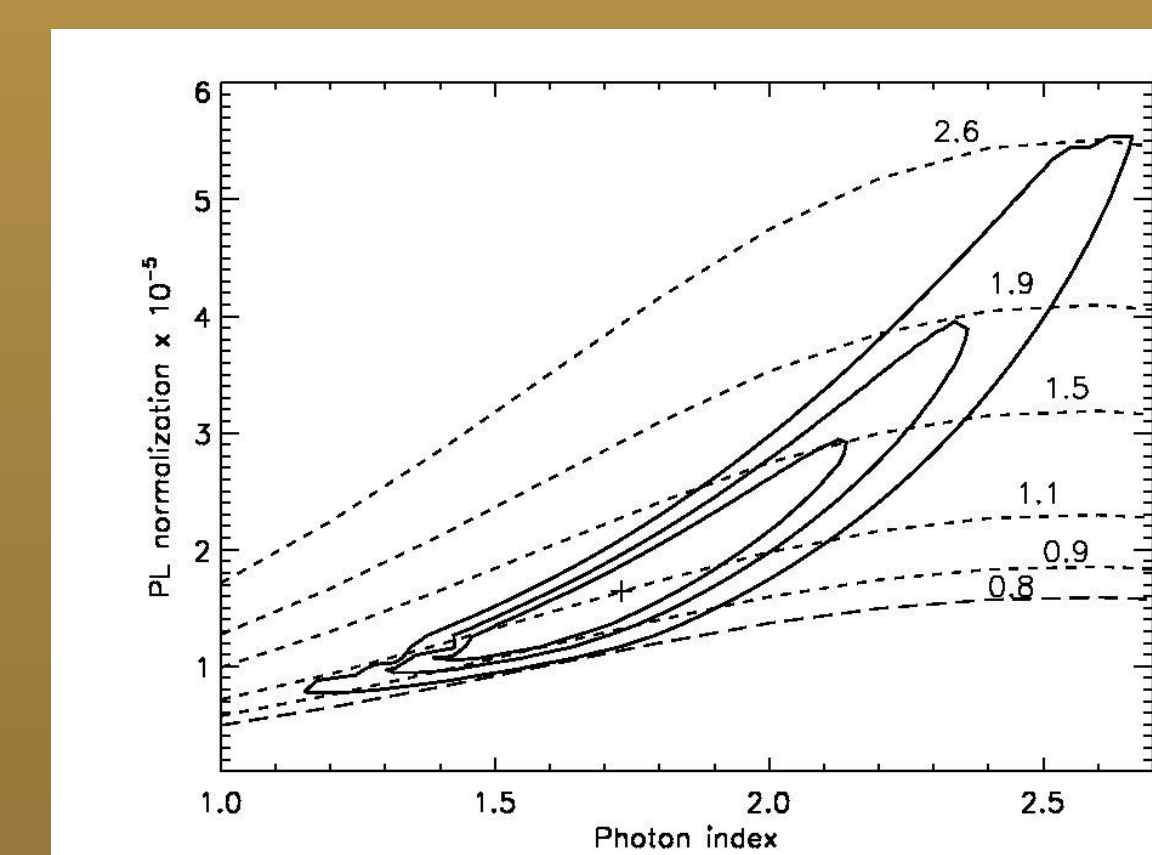
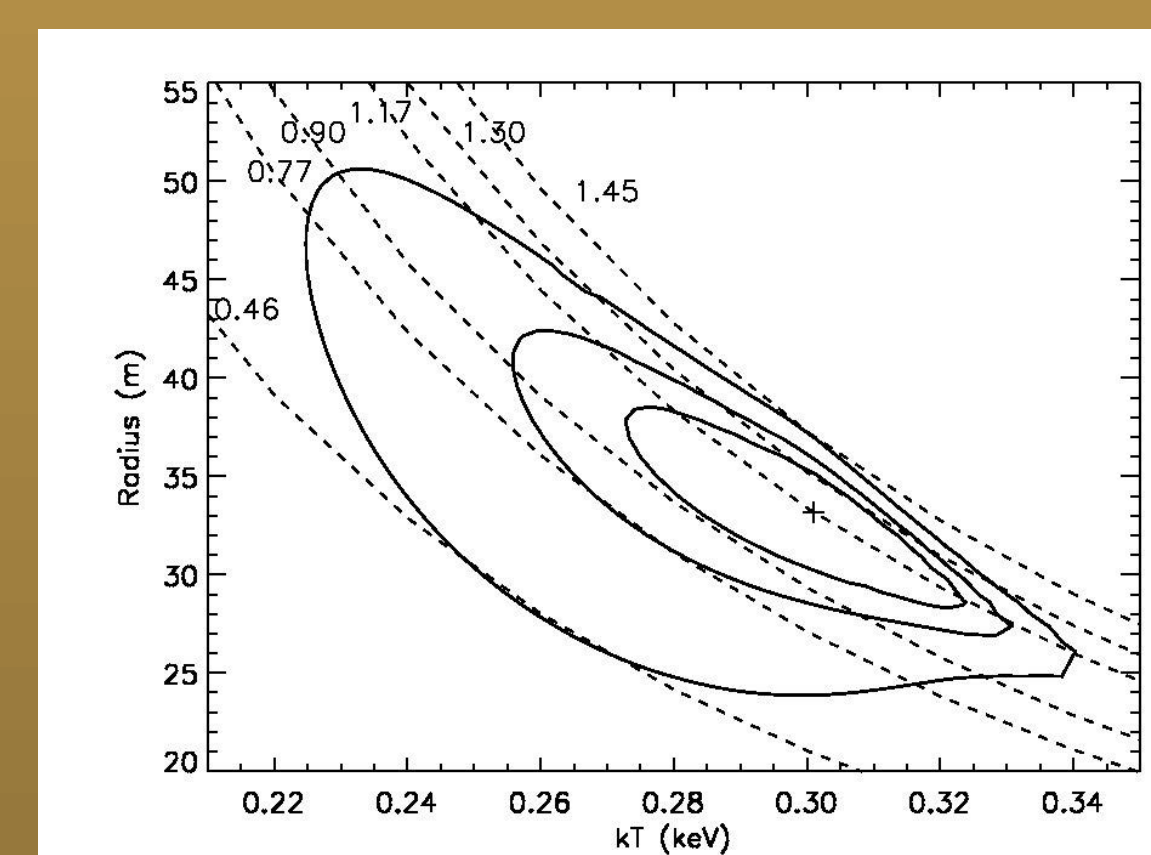
PN, MOS1, and MOS2 spectra of B1929 extracted from the three XMM-Newton observations and fitted simultaneously with the Chandra data using the best-fit absorbed PL+BB model. The model parameters are given in the Table.



Model	N_{H}	Γ	PL Norm	kT	R	χ^2_{dof}	Absorbed Flux	Unabsorbed Luminosity
	10^{21}cm^{-2}		$10^{-14} \text{erg cm}^{-2} \text{s}^{-1} \text{keV}^{-1}$	keV	m		$10^{-14} \text{erg cm}^{-2} \text{s}^{-1}$	$10^{30} \text{erg s}^{-1}$
Chandra								
PL	0.44 $^{+0.02}_{-0.02}$	1.70 $^{+0.05}_{-0.05}$	7.99 $\times 10^{-15}$	0.30 $^{+0.01}_{-0.01}$	33.0 $^{+1.0}_{-1.0}$	0.9571	1.32 $^{+0.03}_{-0.03}$	4.50
PL+BB	0.44 $^{+0.02}_{-0.02}$	1.62 $^{+0.05}_{-0.05}$	1.01 $\times 10^{-14}$	0.30 $^{+0.01}_{-0.01}$	33.0 $^{+1.0}_{-1.0}$	0.9569	1.29 $^{+0.03}_{-0.03}$	4.46
XMM-Newton								
PL	0.22 $^{+0.01}_{-0.01}$	0.90 $^{+0.05}_{-0.05}$	6.96 $\times 10^{-15}$	0.30 $^{+0.01}_{-0.01}$	0.9700	1.86 $^{+0.03}_{-0.03}$	7.98	
PL+BB	0.22 $^{+0.01}_{-0.01}$	1.07 $^{+0.05}_{-0.05}$	1.41 $\times 10^{-14}$	0.30 $^{+0.01}_{-0.01}$	0.9408	1.62 $^{+0.03}_{-0.03}$	3.47	
combined								
PL	0.22 $^{+0.01}_{-0.01}$	1.07 $^{+0.05}_{-0.05}$	6.41 $\times 10^{-15}$	0.30 $^{+0.01}_{-0.01}$	1.0966	1.84 $^{+0.03}_{-0.03}$	6.40	
PL+BB	0.17 $^{+0.01}_{-0.01}$	1.17 $^{+0.05}_{-0.05}$	1.64 $\times 10^{-14}$	0.30 $^{+0.01}_{-0.01}$	0.9969	1.70 $^{+0.03}_{-0.03}$	2.86	

Notes: — The observed flux and unabsorbed luminosity are calculated for the 0.3–10 keV energy band for Chandra, and 0.3–10 keV for XMM-Newton and combined data. The fitted parameters are at 68% confidence level (obtained for 2 interesting parameters). Errors of flux and luminosity are the 1 σ errors of the fit and from the model. Check the last digits for any calculation given. Parameters: 6.630 instead of 6.620 for the combined data. A: Check because you calculated it for the model, and I determined it with XSPEC for the actual data. Hence, the small difference.

Best-fit BB+PL model and its parameters. The contribution of the thermal component is estimated to be ~40-50% of the total X-ray luminosity in the 0.3-8 keV band.



68%, 90%, and 99% confidence contours for various parameters of the best-fit PL+BB model of B1929+10. The contours are computed for the two interesting parameters. The Chandra ACIS-S and XMM-Newton spectra are fitted simultaneously with all parameters left to vary. The left panel shows the lines of constant bolometric luminosity in units 10e30 ergs/s for the thermal component, while the middle panel shows the lines of constant unabsorbed flux in units of 10e-13 ergs/cm^2 s for the PL component.